The Influence of Cobalt, Tantalum, and Tungsten on the Elevated Temperature Mechanical Properties of Single Crystal Nickel-Base Superalloys

M. V. NATHAL and L. J. EBERT

The influence of composition on the tensile and creep strength of [001] oriented nickel-base superalloy single crystals at temperatures near 1000 °C was investigated. Cobalt, tantalum, and tungsten concentrations were varied according to a matrix of compositions based on the single crystal version of MAR-M247.* For alloys with the baseline refractory metal level of 3 wt pct Ta and 10 wt pct W, decreases in Co level from 10 to 0 wt pct resulted in increased tensile and creep strength. Substitution of 2 wt pct W for 3 wt pct Ta resulted in decreased creep life at high stresses, but improved life at low stresses. Substitution of Ni for Ta caused large reductions in tensile strength and creep resistance, and corresponding increases in ductility. For these alloys with low Ta plus W totals, strength was independent of Co level. The effects of composition on properties were related to the microstructural features of the alloys. In general, high creep strength was associated with high levels of γ' volume fraction, γ-γ' lattice mismatch, and solid solution hardening.

I. INTRODUCTION

TRENDS in nickel-base superalloy development have resulted in alloys with as many as a dozen elemental additions, each with its own purpose, to produce a balance of good mechanical properties and environmental resistance.[1] Some recent investigations have involved the roles of strategic materials such as Co[2,3,4] and Ta[5] in a number of superalloys. The present investigation is directed toward examining the influence of both Co and Ta on the elevated temperature tensile and creep-rupture properties of nickel-base superalloy single crystals. These properties will be discussed in relation to the observed microstructural features which were presented in the previous paper.[6] Among the microstructural variables considered were the volume fraction, distribution, morphology, and coarsening rate of the γ' phase, the γ-γ' lattice mismatch, and the composition of both γ and γ'.

II. MATERIALS AND PROCEDURES

Table I presents the nominal concentrations of the intentionally varied elements for the eight single crystal compositions. A more complete description of the compositions, heat treatments, and microstructures can be found in the previous paper.[6] These compositions are based on MAR-M247 (Alloy G), which contains 3 pct Ta, 10 pct W, and 10 pct Co. Alloys B, E, and G are 0, 5, and 10 pct Co alloys at the baseline refractory metal level of 3 pct Ta and 10 pct W. Nickel was substituted for Ta to form alloys with 0 pct Ta and 9 pct W at each Co level: Alloys A, D, and F. Finally, 2 pct W was substituted for 3 pct Ta to form alloys with 0 pct Ta and 12 pct W at 0 and 10 pct Co: Alloys C and H.

Table I. Nominal Compositions* of Alloys

Alloy	Cobalt	Tantalum	Tungsten
A	0	0	9
B	0	3	10
C	0	0	12
D	5	0	9
E	5	3	10
F	10	0	9
G	10	3	10
H	10	0	12

Note: *All values in weight percent. The following elements remained constant at levels appropriate for MAR-M247: Al = 5.5, Cr = 8.5, Ti = 1.0, Mo = 0.7, Ni = balance. Actual compositions are presented in Reference 6.

The single crystal castings were produced by the withdrawal process in the production facilities of TRW, Inc.

All mechanical tests were performed on specimens with gage dimensions of 20 mm length and 4.5 mm diameter. The longitudinal axes of all specimens were oriented within 10 deg of [001]. Tensile tests were performed in air at 1000 °C. The tensile tests were performed with an Instron testing machine at constant crosshead speed, with an initial strain rate of 2.2×10^{-4} s^{-1}. Creep-rupture tests were performed in air at 925 and 1000 °C. Temperature was controlled to ± 1 °C with the aid of two Pt/Pt-13Rh thermocouples attached to the specimens. Loads were applied using 10:1 or 20:1 constant load lever arms. Creep strain was measured using linear variable differential transformers in conjunction with extensometers. The knife edges of the extensometers were placed in grooves machined in the shoulders of the specimen.

III. RESULTS AND DISCUSSION

A. *Results*

1. *Tensile properties*

The 0.2 pct offset yield stress is plotted *vs* Co content in Figure 1. In the baseline 3Ta-10W alloys, reduction in Co

*MAR-M is a trademark of Martin Marietta Company.

M. V. NATHAL, Research Metallurgist, is with NASA Lewis Research Center, Cleveland, OH 44135. L. J. EBERT, Professor of Metallurgy and Materials Science, is with Case Western Reserve University, Cleveland, OH 44106.

Manuscript submitted November 15, 1984.

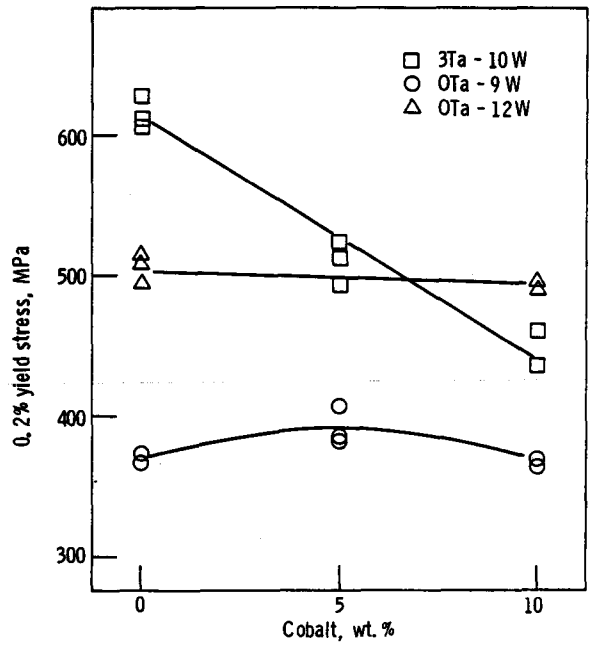

Fig. 1—The 0.2 pct yield stress at 1000 °C for the single crystal alloys.

level from 10 to 0 pct increased the yield stress by a factor of approximately 1.4. Removal of 3 pct Ta and 1 pct W reduced the yield stress by as much as 200 MPa, and the strengths were independent of Co content. Substitution of 2 pct W for the baseline 3 pct Ta slightly increased the strength at the 10 pct Co level, but caused a reduction in strength at the 0 pct Co level. The ultimate tensile strengths of the crystals exhibited similar results, as evident in Figure 2. For the 3Ta-10W series of alloys, the ultimate tensile stress increased by a factor of about 1.3 as Co level decreased from 10 to 0 pct, whereas the 0Ta-9W alloys possessed ultimate strengths about 15 pct lower than the

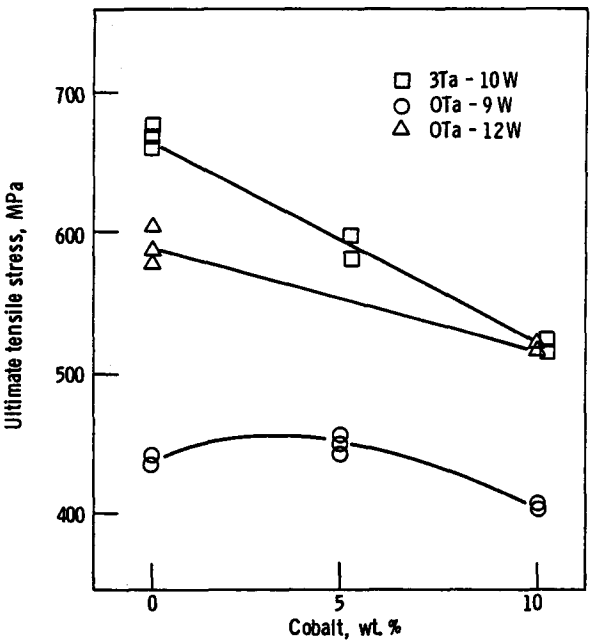

Fig. 2—The ultimate tensile strength at 1000 °C for the single crystal alloys.

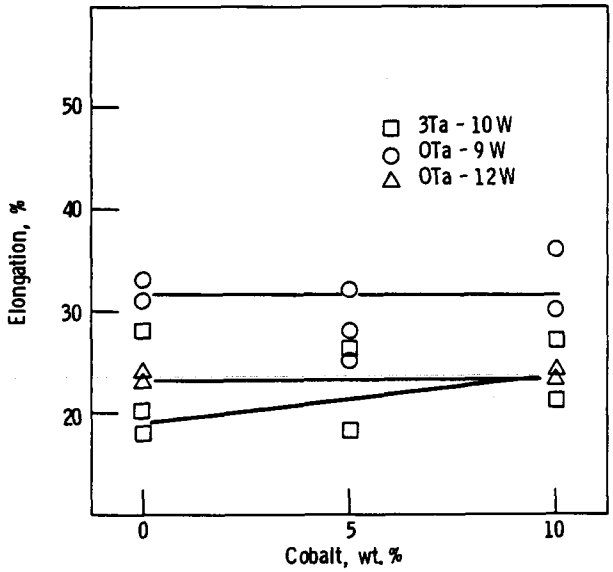

Fig. 3—Tensile ductilities at 1000 °C for the single crystal alloys.

baseline alloy. The partial substitution of W for Ta did not affect the strength of the 10 pct Co alloy, but caused a reduction in strength by about a factor of 1.2 in the 0 pct Co alloy.

The tensile ductilities of the alloys are shown in Figure 3. Both percentage reduction in area and percentage elongation were higher for the lower strength alloys. For example, the 0Ta-9W alloys possessed the lowest yield and tensile strengths, but had the highest tensile ductilities, approximately 30 pct elongation. The lowest elongation value of about 20 pct was measured for the highest strength Alloy B.

2. *Creep-rupture properties*

Extensive creep-rupture testing was performed at 1000 °C over a range of stresses. In addition, a limited amount of testing was performed at 925 °C. At 1000 °C, Alloy B, also known as NASAIR 100, exhibited typical three-stage creep behavior, which consisted of a "normal" primary creep stage whereby the creep rate gradually decreased to the steady state value.[7] The second stage creep region was characterized by a constant creep rate over an extended period, followed by a gradual increase in creep rate as the tertiary creep stage commenced. The creep curves for the other seven alloys were similar to those of Alloy B except for the primary creep stage. These alloys exhibited an incubation period of very low creep rate before a sigmoidal-shaped primary stage, as exemplified by Alloy E in Figure 4. The duration of the incubation period was typically 2 hours. No trends in the durations of the incubation period as a function of applied stress or alloy composition were noted.

The creep ductilities of the alloys followed trends similar to the trends in the tensile ductilities. Typically, alloys with high creep resistance exhibited lower creep ductility. No trends in ductility as a function of stress level were apparent. Alloy C, with the highest creep resistance, had the lowest ductility of approximately 13 pct elongation. The 0Ta-9W alloys exhibited the lowest creep strength and the highest creep ductilities, possessing elongation values near 35 pct.

The steady state creep rate, $\dot{\varepsilon}_s$, the time to failure, t_f, the time to the onset of tertiary creep, t_t, and the time to

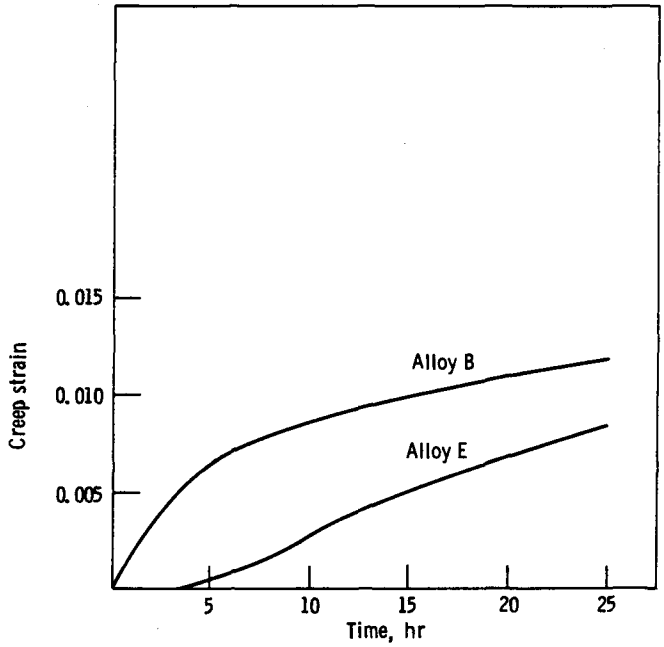

Fig. 4 — Primary creep curves for Alloys B and E at 1000 °C and 207 MPa.

the onset of secondary creep, t_s, were measured for all tests. The data of all alloys were plotted as a function of applied stress. The following equations were fitted by standard regression techniques, where A_1 through A_5 are constants and k, l, m, n, and p are the stress exponents:

$$\dot{\varepsilon}_s = A_1\sigma_a^n \quad [1]$$

$$t_f = A_2\sigma_a^{-p} \quad [2]$$

$$t_t = A_3\sigma_a^{-l} \quad [3]$$

$$t_s = A_4\sigma_a^{-k} \quad [4]$$

$$\dot{\varepsilon}_s = A_5 t_f^{-m} \quad [5]$$

Equations [1] through [4] express the various parameters as power law functions of the applied stress. Equation [5] is a form of the Monkman-Grant relationship,[8] which relates the steady state creep rate to the rupture life. Double logarithmic plots of $\dot{\varepsilon}_s$ and t_f *vs* applied stress are presented in Figures 5 and 6. The data, in addition to similar plots for the other parameters, consistently exhibited linear behavior, which supports the use of the power law relations in Eqs. [1] through [5]. The slopes of these plots, which are equal to the stress exponents in Eqs. [1] through [5], are presented in Table II. The creep rate exponent n is consistently greater than the rupture life exponent p. The exponent l, which relates the onset of tertiary creep to the applied stress, consistently falls between n and p. In addition, the values of n and p are relatively constant as a function of alloy composition.

The summary plots of creep rate and rupture life, Figures 5(d) and 6(d), respectively, indicate some of the trends in creep behavior as a function of composition. For the 3Ta-10W alloys (G, E, and B), the steady state creep rate was reduced by approximately a factor of 5 as Co content was reduced from 10 to 0 pct. This trend was consistent for all stress levels. For the 0Ta-12W alloys (C and H), similar trends were observed whereby reduction of Co level from 10 to 0 pct caused a reduction in creep rate by about a factor of 5 at high stresses and a factor of 8 at low stresses. The influence of Co in the creep rates of the 0Ta-9W alloys was not very strong, where the differences were all within a factor of two.

Although the 0Ta-9W alloys always possessed higher creep rates than the other alloys, independent of stress level, the relative ranking of the 0Ta-12W and 3Ta-10W alloys was a function of the applied stress. For example, the 0Ta-12W Alloy C exhibited a higher creep rate than that of the 3Ta-10W Alloy B at high stresses. However, the higher stress dependence exhibited by Alloy C resulted in a crossover in strength such that the creep rate of Alloy C was lower than that of Alloy B at stresses below approximately 200 MPa.

The rupture lives of the alloys followed trends consistent with the trends in creep rates, *i.e.*, alloys with higher steady state creep rates had shorter rupture lives. For the baseline refractory metal alloys, removal of Co caused an increase in life by about a factor of 1.5, as presented in Figure 6(d). Removal of Co from the 0Ta-12W alloys resulted in increases in life by a factor of 2.4 at 148 MPa and a factor of 2 at 207 MPa. The influence of Co was much smaller for the 0Ta-9W alloys, as the lives of Alloys A, D, and F were all within a factor of 1.2. The influence of refractory metal level on rupture life also correlated with the trends exhibited by the creep rate data. The 0Ta-9W alloys possessed shorter lives at all stress levels, in comparison to the higher refractory metal alloys. Again, the 0Ta-12W alloys exhibited a higher stress dependence than the 3Ta-10W alloys, which resulted in a crossover in rupture lives. At high stresses, the 3Ta-10W alloys possessed longer lives, whereas at lower stresses, the 0Ta-12W alloys lasted longer.

Table II. Creep-Rupture Exponents

Alloy	$\dot{\varepsilon}_s = A_1\sigma^n$ n	$t_f = A_2\sigma^{-p}$ p	$t_t = A_3\sigma^{-l}$ l	$t_s = A_4\sigma^{-k}$ k	$\dot{\varepsilon}_s = A_5 t_f^{-m}$ m
A	8.37 ±2.94*	6.24 ±1.74	7.34 ±2.66	3.15 ±1.52	1.34 ±0.36
B	7.60 ±0.60	5.87 ±0.33	6.84 ±0.30	5.30 ±0.90	1.13 ±0.11
C	10.60 ±1.33	7.21 ±0.65	8.15 ±0.59	5.32 ±0.82	1.47 ±0.14
D	8.27 ±0.69	6.03 ±0.76	7.37 ±1.12	4.30 ±4.00	1.37 ±0.27
E	7.91 ±2.45	5.15 ±1.68	6.35 ±1.76	3.59 ±2.83	1.50 ±0.42
F	7.51 ±0.90	5.66 ±0.59	5.83 ±1.72	4.67 ±4.14	1.32 ±0.24
G	6.42 ±1.15	5.18 ±1.03	5.68 ±1.37	5.32 ±2.90	1.22 ±0.43
H	9.46 ±1.62	6.77 ±0.45	7.82 ±0.54	4.93 ±2.78	1.40 ±0.17

Note: * 95 pct confidence intervals

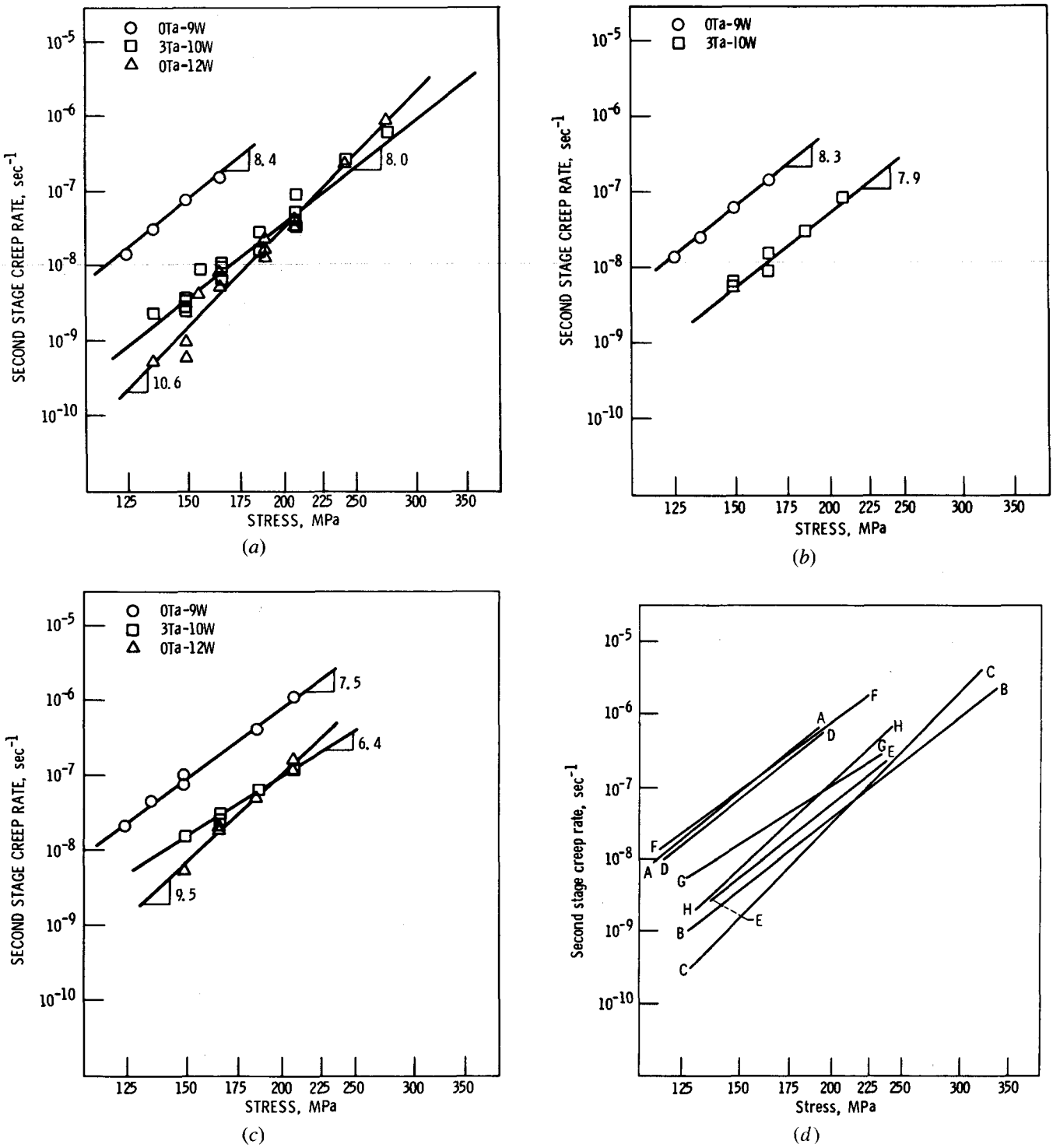

Fig. 5 — Stress dependence of the steady state creep rates of the single crystal alloys at 1000 °C: (*a*) 0 pct Co alloys, (*b*) 5 pct Co alloys, (*c*) 10 pct Co alloys, and (*d*) summary plot with all alloys.

The composition effects can be more easily seen in Figure 7, a plot of rupture life *vs* composition at 1000 °C and 148 MPa. A decrease in Co content from 10 to 0 pct in the 3Ta-10W alloys produced an increase in rupture life from 435 to 790 hours. Substitution of 2 pct W for 3 pct Ta increased the rupture life at both Co levels, although the effect was greater at 0 pct Co. The rupture life increased from 790 to 1322 hours upon the W substitution for Ta in the 0 pct Co alloy and from 435 to 544 hours for the 10 pct Co alloy. Also evident in Figure 7 is that the 0Ta-9W alloys were by far the weakest in creep resistance at all Co levels.

The similar trends of creep rate and rupture life with composition imply a close correlation between creep rate and rupture life, which is supported by the excellent fit of

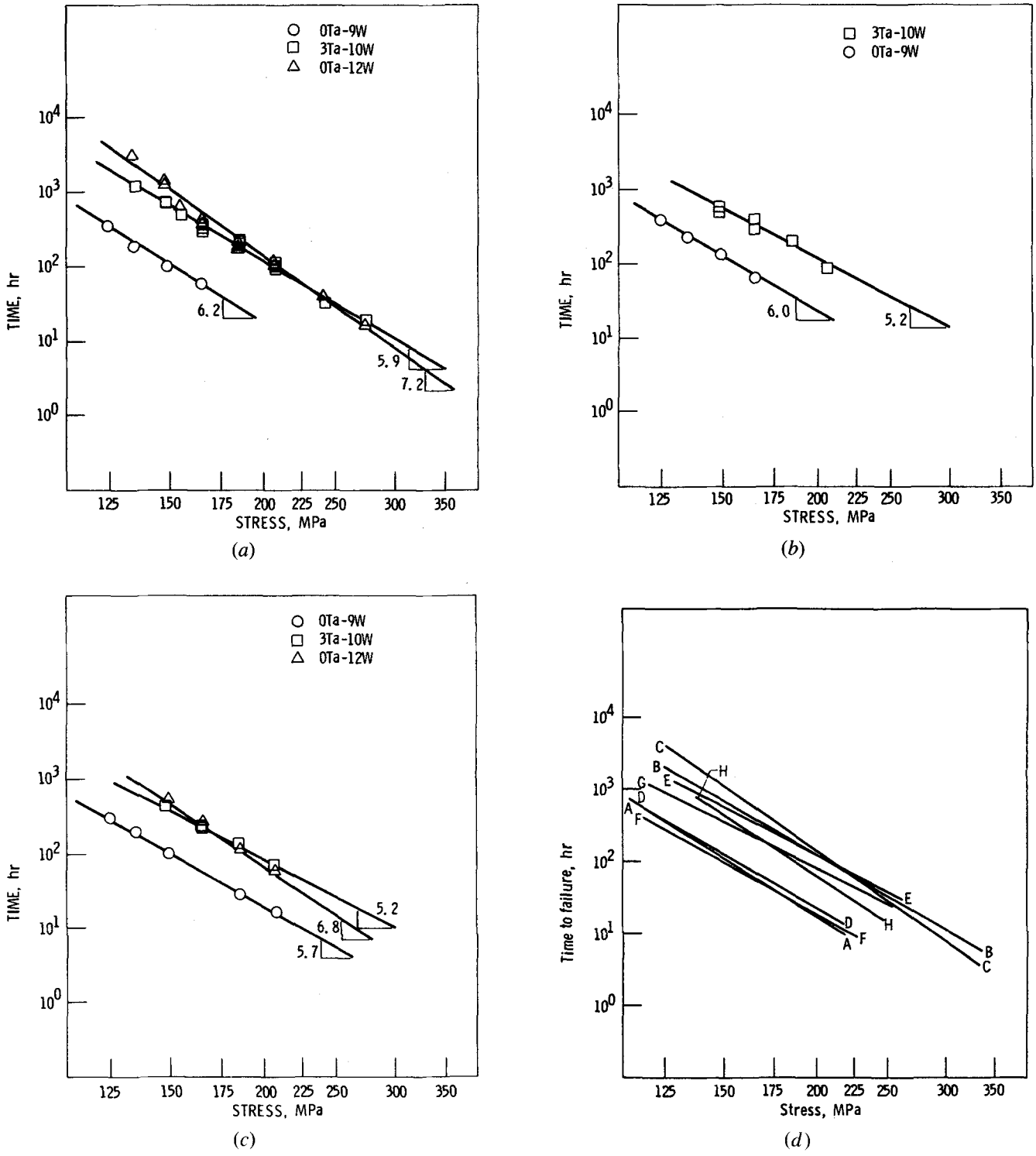

Fig. 6—Stress dependence of the rupture lives of the single crystal alloys at 1000 °C. (*a*) 0 pct Co alloys, (*b*) 5 pct Co alloys, (*c*) 10 pct Co alloys, and (*d*) summary plot with all alloys.

the data by the Monkman-Grant relationship, Eq. [5]. The values of the exponent m, presented in Table II, were approximately constant for all alloys. The values of m were close to but significantly greater than one, a value frequently observed in other materials.

Finally, limited testing was performed at 925 °C. Figure 8 displays the rupture lives of several alloys at 925 °C and 207 MPa. The 0Ta-9W alloys were again the least creep-rupture resistant alloys, but all the alloys with high Ta plus W totals exhibited lives within 20 pct of each other. Comparison of the data in Figure 8 with that in Figure 7 reveals that the slight trend of decreasing life at 925 °C as Co content was reduced was the reverse of the trend exhibited by these alloys at 1000 °C. In light of the crossover behavior between the 0Ta-12W and 3Ta-10W alloys at 1000 °C, more extensive testing at 925 °C would be

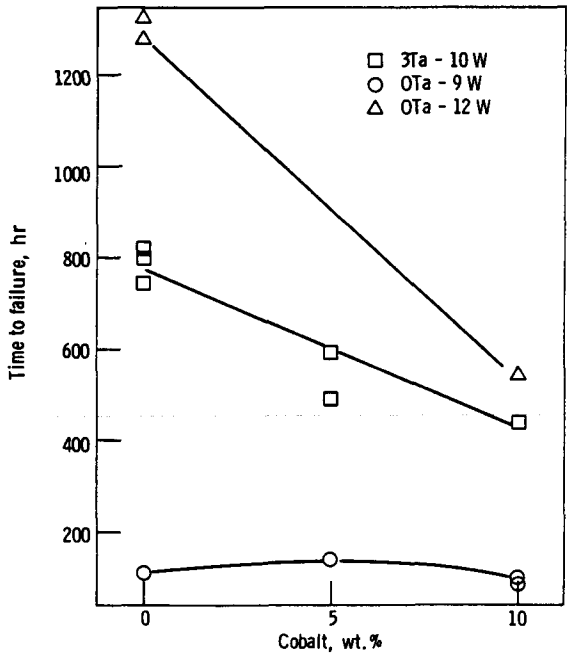

Fig. 7—Rupture lives of the single crystal alloys at 1000 °C and 148 MPa.

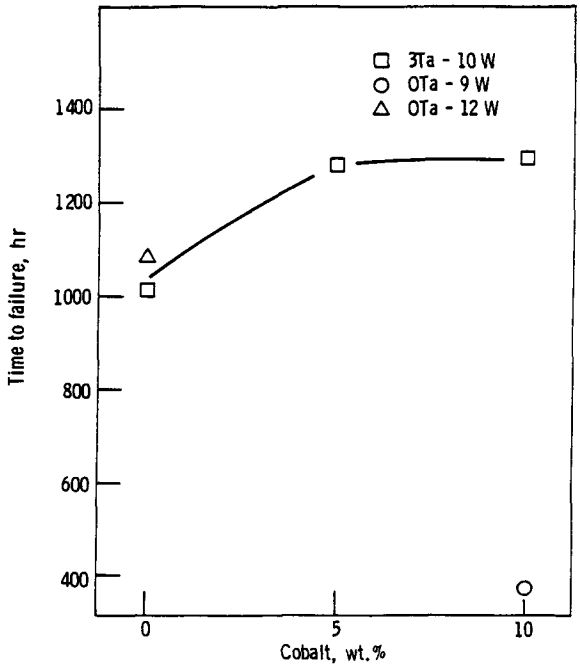

Fig. 8—Rupture lives of the single crystal alloys at 925 °C and 207 MPa.

required to characterize satisfactorily the behavior at this temperature.

B. *Discussion*

The effects of the Co, Ta, and W variations on the microstructure of the single crystal alloys are described in detail elsewhere[6] and will be listed only briefly here. Reduction of Co from 10 to 0 pct did not affect the γ' volume fraction, but did cause an increase in the magnitude of lattice mismatch for the alloys with high Ta plus W totals. Substitution of Ni for Ta caused large reductions in γ-γ' lattice mismatch and γ' volume fraction, and substitution of W for Ta caused intermediate reductions in mismatch and γ' volume fraction. Alloys with 0 pct Co and high refractory metal levels also exhibited precipitation of the W-rich phases α and μ. For alloys with γ' particles that remained coherent, reduction of Co content increased the unstressed γ' coarsening rate. During creep, all alloys exhibited directional γ' coarsening to form lamellae perpendicular to the applied stress. Alloys with higher magnitudes of lattice mismatch exhibited faster directional coarsening rates and finer spacings of misfit dislocations at the γ-γ' interfaces.

1. *Tensile properties*

The strength of superalloys results from a number of strengthening mechanisms such as solid solution hardening, order hardening, and coherency hardening. Alloying changes would be expected to influence all of the above mechanisms. The dependence of yield and ultimate tensile strength on composition was primarily related to the Ta plus W totals. The strong influence of Ta and W levels on strength can be discussed in general terms by the contribution of these elements to solid solution and precipitation strengthening. However, solid solution strengthening of γ and γ', lattice mismatch, and the volume fraction of γ' are all affected by the refractory element level. Thus it is not possible to separate the relative contributions of these mechanisms. The strong influence of Co content on the strength of the baseline 3Ta-10W alloys can be explained by the increased γ-γ' lattice mismatch as Co level was reduced.[6] The increased misfit would increase the contribution of coherency strain hardening to the strength of these alloys.

2. *Creep-rupture properties*

The similarities in creep curves, stress exponents, microstructure, and composition among the alloys imply that the creep deformation mechanisms are also similar. The creep behavior of Alloy B was studied in greater detail,[7] and a summary of the observed behavior is provided below. At 1000 °C, the γ' particles rapidly coalesced into lamellae perpendicular to the applied stress. This lamellar structure prevented dislocation bypassing of the γ' phase, thus forcing the dislocations to shear through the lamellae, where it appears likely that shear through the γ-γ' interface is the most difficult step. A hexagonal array of misfit dislocations was present at the interface, and acted as a barrier to dislocation motion. Strain enhanced thickening of the γ' lamellae resulted in a gradual increase in creep rate as the tertiary creep stage commenced. At 925 °C, the rate of directional coarsening was signficantly slower, and the γ-γ' lamellar structure did not appear to be as influential in the creep processes, since both cuboidal and lamellar γ' structures produced similar lives.

An interesting observation was the occurrence of incubation periods and sigmoidal primary creep curves for seven of the alloys. Incubation periods and sigmoidal creep curves are usually associated with low initial dislocation densities and high dislocation drag stresses,[9] and have been observed in superalloys previously.[10,11] In the case of Alloy B at 1000 °C, the lack of an incubation period and sigmoidal primary region must be the result of some feature providing dislocation sources, such as the higher subgrain boundary density observed in Alloy B. However, another feature that can explain the high initial creep rates is the rapid directional

γ' coarsening exhibited by Alloy B.[6] The directional coarsening is accompanied by a rapid generation of misfit dislocations, which can result in significant accumulation of primary creep strain if the generation of misfit dislocations occurs by the punching mechanism described by Weatherly and Nicholson.[12,13] The lower mismatch values of the other alloys, however, results in much slower directional coarsening, and would make the punching mechanism less likely. It is likely that the γ' particles of these alloys acquired their misfit dislocations at a slower rate by the capture of dislocations from matrix sources. Incubation periods and sigmoidal primary creep curves would then result from the slower γ' coarsening and the lack of a mechanism for rapid generation of dislocations.

The influences of alloy composition on the creep-rupture properties can be discussed in relation to the creep behavior and microstructural observations mentioned above. The reductions in creep resistance as Ni was substituted for Ta were expected, and can be explained by the reductions in γ' volume fraction and solid solution hardening as Ta level was decreased. These are the same arguments used to explain the decreases in tensile strength caused by the same alloying changes. The term "solid solution hardening" is used to include all of the effects of the solute atoms, including modulus, stacking fault energy, APB energy, and diffusion.

The decreases in creep resistance as Co level increased in the 3Ta-10W and 0Ta-12W alloys are not as easily related to the tensile behavior. The increases in tensile strength as Co level decreased from 10 to 0 were rationalized by the increased contribution of coherency strain hardening caused by the increase in lattice mismatch. However, this argument may not apply to longer term testing, whereby the effects of microstructural instabilities may become more important. Many authors have suggested that higher mismatch values may decrease life by enhancing γ' coarsening and thus overaging.[1,14,15]

For the alloys in the present study, high γ-γ' lattice mismatch can actually improve creep resistance. The beneficial effects of high mismatch involve the increased barrier to dislocation motion from either elastic coherency strains or the finer spacing of misfit dislocations. The negative effect of high mismatch, which would be a higher γ' coarsening rate, is minimized in the present case. Increased mismatch does cause very rapid directional γ' coarsening, but only in the initial portions of the creep test. The rapid directional coarsening observed in the present study did not cause the typical overaging response whereby dislocation bypassing mechanisms become easier as the particles grow. In contrast, the formation of the lamellae suppressed the bypassing mechanisms.[7,16,17]

Once formed, the γ' lamellae coarsen only very slowly during the remainder of the creep life. Lower mismatch values can actually increase the plate thickening which occurs during the later stages of the creep test. As previously discussed, this thickening appears to be enhanced by creep strain.[7] Therefore, a lower mismatch would result in a smaller barrier to dislocation flow, and would cause a higher steady state creep rate. This higher strain rate would therefore enhance the plate thickening rate, which in turn would result in an earlier onset of tertiary creep and failure.

Finally, a fine array of misfit dislocations may also contribute to the stability of the γ' lamellae by reducing the mobility of the interface. An indication of the stabilizing effect of misfit dislocations on γ' coarsening was also seen in the Ostwald ripening experiments, where Alloys B and C were the only alloys that lost coherency during coarsening, and exhibited anomalously low coarsening rates.[6]

The influence of Co on the present alloys supports the postulate that high lattice mismatch is beneficial for creep properties. The effects of Co cannot be attributed to solid solution hardening by Co, because the Co additions actually decreased the creep resistance of the 0Ta-12W and 3Ta-10W alloys. Furthermore, the presence of α and μ phases in the 0 pct Co Alloys B and C reduced the amount of W available for precipitation and solid solution hardening compared to the alloys with 5 and 10 pct Co. Again, this effect would be expected to increase the strength of the 5 and 10 pct Co alloys if it would have any effect at all. Thus, it appears likely that the decreases in creep resistance with increasing Co level was not caused by decreases in strength of the individual phases. However, the strength of the γ-γ' interface, as measured by the lattice mismatch, was strongly influenced by Co content. The higher mismatch would decrease the spacing of the hexagonal misfit dislocation array, and therefore strengthen the lower Co alloys. The increase in lattice mismatch can therefore account for the increased creep resistance of these alloys as Co level was decreased.

The influence of the substitution of W for Ta on the creep properties of the single crystal alloys was more puzzling. For example, Alloy C had a slightly lower γ' volume fraction, γ-γ' mismatch, and Ta plus W total than Alloy B, all of which would be expected to weaken Alloy C in comparison to Alloy B. In fact, these features may be the reasons for the results of the short term tests, where Alloy B was indeed stronger. However, some other microstructural feature must cause the observed crossover in creep resistance at lower applied stresses. One could argue that Alloy C exhibited better creep resistance at low stresses because it possessed smaller amounts of W-rich phases than Alloy B. However, this could not explain the same trends in strength at 10 pct Co, where both Alloys H and G were free of any third phases. One possibility is that the W is more effective as a solid solution hardener than Ta. Thus, a possible explanation for the crossover in strength exhibited between the 0Ta-12W and 3Ta-10W alloys is provided. At high applied stresses, the slight decreases in volume fraction and mismatch causes the 0Ta-12W alloys to be less resistant to plastic flow. At progressively lower stresses, solid solution strengthening becomes more important, which results in the crossover in creep strength. However, only limited data are available on the influence of alloying on the various mechanisms by which a solute atom may improve creep resistance, and it is recognized that further study is necessary to establish the influence of refractory metals on the creep properties of superalloys.

The creep processes at the lower temperatures of 925 °C did not appear to be totally analogous to the processes at 1000 °C. The results on the study of Alloy B[7] indicated that the γ-γ' lamellar structure did not appear to be beneficial at the lower temperature. In addition, the influence of composition was different at the two temperatures. The effects of Co level, which were so prominent at 1000 °C, were reduced and possibly even reversed at 925 °C, and the substitution of W for Ta also did not affect the creep properties

as significantly. These data also suggest that the creep mechanisms are different at the lower temperature. More extensive testing is required to clarify the creep processes at 925 °C.

IV. CONCLUSIONS

1. The steady state creep rate, time to failure, time to the onset of secondary creep, and the time to the onset of tertiary creep all exhibited power law dependencies on the applied stress. The stress exponent for the steady state creep rate was approximately 8 for all alloys, although some small but significant differences between alloys did exist.
2. Substitution of Ni for Co caused large increases in creep resistance for alloys with high Ta plus W totals. This was consistent with an increase in γ-γ' lattice mismatch. High values of lattice mismatch resulted in a finer dislocation network at the γ-γ' interface, thus providing a more effective barrier for dislocation motion. Substitution of Ni for Ta and W to form the 0Ta-9W alloys caused large reductions in creep resistance, which were related to the decreases in γ' volume fraction, γ-γ' mismatch, and solid solution hardening. Substitution of W for Ta to form the 0Ta-12W alloys resulted in a decrease in creep resistance at high stresses and an increase in creep strength at low stresses. This crossover in creep resistance between the 3Ta-10W and 0Ta-12W alloys was not easily explained. The decreased life of the 0Ta-12W alloys at high stresses was attributed to the slight decreases in γ' volume fraction and γ-γ' mismatch, although it remains unclear as to why W appears to be a more effective solid solution strengthener than Ta at low stresses.
3. Decreases in Co level from 10 to 0 pct caused significant increases in the 1000 °C yield and ultimate tensile strengths of the 3Ta-10W alloys, but the effect of Co was much less for alloys with other refractory metal contents. The influence of Co on the strength of the 3Ta-10W alloys was attributed to coherency strain hardening associated with the increased lattice mismatch as Co level decreased. Reduction of Ta and W content to form the 0Ta-9W alloys caused large reductions in tensile strength, and substitution of W for Ta caused intermediate decreases in strength. These changes in tensile strength with refractory metal level were related to the increases in γ' volume fraction and solid solution hardening which resulted from high Ta plus W totals.

REFERENCES

1. R. F. Decker: in *Steel Strengthening Mechanisms Symposium*, Climax Molybdenum Co., Greenwich, CT, 1969, p. 147.
2. G. E. Mauer, L. A. Jackman, and J. A. Domingue: in *Superalloys 1980, Proc. 4th Intl. Sym. on Superalloys*, J. K. Tien, S. T. Wlodek, H. Morrow, M. Gell, and G. E. Mauer, eds., ASM, Metals Park, OH, 1980, p. 43.
3. R. N. Jarrett and J. K. Tien: *Metall. Trans. A*, 1982, vol. 13A, p. 1021.
4. M. V. Nathal, R. D. Maier, and L. J. Ebert: *Metall. Trans. A*, 1982, vol. 13A, p. 1767.
5. H. C. Nguyen, B. J. Pletka, and R. W. Heckel: in *High Temperature Alloys: Theory and Design*, J. O. Stiegler, ed., AIME, Warrendale, PA, 1984, p. 381.
6. M. V. Nathal and L. J. Ebert: *Metall. Trans. A*, 1985, vol. 16A, p. 1849.
7. M. V. Nathal and L. J. Ebert: *Metall. Trans. A*, 1985, vol. 16A, p. 427.
8. F. C. Monkman and N. J. Grant: *Proc. ASTM*, 1956, vol. 56, p. 834.
9. P. R. Strutt and R. A. Dodd: in *Ordered Alloys: Structural Applications and Physical Metallurgy*, B. H. Kear, C. T. Sims, N. S. Stoloff, and J. H. Westbrook, eds., Claitor's Publishing, Baton Rouge, LA, 1969, p. 475.
10. G. R. Leverant and B. H. Kear: *Metall. Trans.*, 1970, vol. 1, p. 491.
11. C. Carry and J. L. Strudel: *Acta Metall.*, 1978, vol. 26, p. 859.
12. G. C. Weatherly and R. B. Nicholson: *Phil. Mag.*, 1968, vol. 17, p. 801.
13. G. C. Weatherly: *Phil. Mag.*, 1968, vol. 17, p. 791.
14. N. S. Stoloff: in *The Superalloys*, C. T. Sims and W. C. Hagel, eds., John Wiley and Sons, Inc., New York, NY, 1972, p. 79.
15. R. G. Davies and T. L. Johnson: in *Ordered Alloys: Structural Applications and Physical Metallurgy*, B. H. Kear, C. T. Sims, N. S. Stoloff, and J. H. Westbrook, eds., Claitor's Publishing, Baton Rouge, LA, 1969, p. 447.
16. D. D. Pearson, F. D. Lemkey, and B. H. Kear: in *Superalloys 1980, Proc. 4th Int. Symp. on Superalloys*, J. K. Tien, S. T. Wlodek, H. Morrow, M. Gell, and G. E. Mauer, eds., ASM, Metals Park, OH, 1980, p. 513.
17. D. D. Pearson, B. H. Kear, and F. D. Lemkey: *Creep and Fracture of Engineering Materials and Structures*, B. Wilshire and D. R. J. Owen, eds., Pineridge Press, Swansea, UK, 1981, p. 213.